Corrosion inhibition of carbon steel in 0.5 M NaCl aqueous solution by humid air plasma treatment

6 authors, including:

Noureddine Ghali
Université Abdelhamid Ibn Badis Mostaganem
2 PUBLICATIONS **7** CITATIONS

SEE PROFILE

Ahmed Addou
Université Abdelhamid Ibn Badis Mostaganem
106 PUBLICATIONS **1,419** CITATIONS

SEE PROFILE

Baghdad Benstaali
Oman Medical College
13 PUBLICATIONS **631** CITATIONS

SEE PROFILE

Fouad Bentiss
National Graduate School of Engineering Chemistry of Lille (ENSCL)
178 PUBLICATIONS **8,905** CITATIONS

SEE PROFILE

Some of the authors of this publication are also working on these related projects:

Testing the corrosion inhibition efficeincy of some new synthetic organic cmpounds on mild steel in acidic media View project

Synthesis of new benzodiazepine and benzimidazole derivatives □and testing their biological activities and corrosion inhibition efficeincy as well. View project

Corrosion inhibition of carbon steel in 0.5 M NaCl aqueous solution by humid air plasma treatment

Noureddine Ghali, Ahmed Addou, Brigitte Mutel, Baghdad Benstaali, Fouad Bentiss, and Jean-Louis Brisset

Regular Article

Corrosion inhibition of carbon steel in 0.5 M NaCl aqueous solution by humid air plasma treatment

Noureddine Ghali[1], Ahmed Addou[1,a], Brigitte Mutel[2], Baghdad Benstaali[1], Fouad Bentiss[3], and Jean-Louis Brisset[4]

[1] Laboratory of Science and Technology Environment and Valorization (STEVA), University of Mostaganem, 27000 Mostaganem, Algeria
[2] Laboratory of Plasma Process and Materials (P2M), UMR CNRS 8520, University of Lille 1, 59655 Villeneuve d'Ascq, France
[3] Laboratory of Polymers Systems Ingeneering, UMR-CNRS 8207, ENSCL, University of Lille 1, 59655 Villeneuve d'Ascq, France
[4] Electrochemistry Laboratory (LEICA), UFR Sciences, University of Rouen, 76821 Mont-Saint-Aignan Cedex, France

Abstract. Carbon steel (C75) is exposed to highly reactive species such as hydroxyl radicals $^\bullet$OH created by a gliding arc discharge (GAD) in humid air at atmospheric pressure. The protective properties of carbon steel treated by GAD are studied versus different treatment times (t) and for an immersion in corroding 0.5 M sodium chloride solution during 24 h. Evolutions of corrosion rate are studied using weight loss measurements and electrochemical methods, e.g., electrochemical impedance spectroscopy (EIS) and potentiodynamic polarization. The results obtained by GAD treatment show that the corrosion rate of steel decreases with the ennoblement of the corrosion potential and the decrease of the corrosion current density. This indicates that the plasma treatment acts as an anodic type inhibitor and suggests the formation of a protective layer. EIS measurements confirm the presence of this film: the charge transfer resistance (R_{ct}) increases with GAD treatment time, leading to a corrosion inhibition efficiency around 73% for a treatment time equal to 60 min. This confirms the importance of the plasma effect. The gliding arc discharge is a clean and efficient technology for the surface treatment of carbon steel; it improves the anticorrosion properties of steel in aggressive environments, forming a resistant and insulating barrier.

1 Introduction

Investment costs related to corrosion inhibition in industrialized countries represent 2–4% of gross national product. Direct or indirect damage caused by the corrosion of metallic materials is very significant. Carbon steel is one of the most important and widely used materials that play a fundamental role in metallurgical industries. Steel with high carbon content is used for applications where high resistance and hardness properties are required such as wearing elements, kitchenware, vehicle gearboxes, saw blades, springs, chains, washers and others. Steel corrosion may occur even in reinforced concrete, if chlorides penetrate through the concrete and reach the steel reinforcement causing the attack of the passive film. The corrosive attack due to chloride penetration usually leads to localized corrosion causing the accelerated loss of the steel section, which may cause rapid failure of the reinforcement barrier [1].

Emerging processes using electrical discharges plasma are used and applied to various fields. The gliding arc discharge (GAD), i.e., a technique that operates close to ambient temperature and atmospheric pressure, has been successfully applied from the degradation of liquid solutes [2–7] to pollutant abatement and surface protection for higher corrosion-resistant stainless steels [8–10]. Plasma treatment nowadays represents an important tool for modifying and improving the chemical and surface properties of solid materials, such as improving the corrosion resistance, etching, and cleaning [11,12], and modifying the surface of material support to affect bacterial adhesion [13]. A GAD in the presence of humid air generates highly oxidizing radicals such as $^\bullet$OH (standard potential $E^\circ(^\bullet OH/H_2O) = 2.85$ V/NHE) and its dimer H_2O_2 [$E^\circ(H_2O_2/H_2O) = 1.68$ V/NHE]. These radicals are responsible for the formation of metal oxides on the treated surface that form a protective barrier layer which enhances the corrosion resistance [14–16]. Other species (e.g., NO and their derivatives, such as peroxynitrite $ONOO^-$) are

a e-mail: a.addou@univ-mosta.dz

formed and participate accordingly in the oxidizing character of the plasma $[E°(ONOO^-/NO_2) = 2.44$ V/NHE] and the formation of oxide layers. Various low temperature plasma treatments have been developed to prevent corrosion of carbon steel [17–20]. However, while the corrosion behavior of structural steels of low carbon is well known, work on steels with high carbon content could not be found in the literature. That is why we focused our study on these types of widely used materials in desalination plants in marine environments. The aim of this work is to enhance the corrosion resistance of carbon steel (C75) by a GAD treatment. After treatment, samples are immersed in corroding solution (25 °C) during 24 h and their corrosion resistance is evaluated using gravimetric, potentiodynamic polarization and electrochemical impedance spectroscopy (EIS) measurements. The influence of pH and of various electrolytes was investigated.

2 Experimental materials and methods

2.1 Materials

2.1.1 Carbon steel

The material used in this study was C75 carbon steel which was provided by Weber Metaux with the following chemical composition (in wt.%) of C: 0.70–0.80, Si: 0.15–0.35, Mn: 0.60–0.90, P: 0.025, S: 0.025, Cr: 0.20–040 and the remainder iron (Fe). For all the experiments, the carbon steel samples were polished with silicon carbide emery (120, 340, 600 and 1200) to produce a fine surface finishing; degreased in ethanol for 10 min in ultrasonic bath and washed with distilled water, degreased in acetone and dried.

2.1.2 Gliding arc discharge (GAD) apparatus

The GAD reactor used for this study (Fig. 1) was proposed by Lesueur et al. [21]. An electric arc ignites at the smallest gap between two diverging electrodes raised to a convenient potential difference. The electric power is provided by a special transformer (50 Hz; 9000 V; 100 mA in open conditions). The electric arc is pushed away from the ignition point by the feeding gas flow. It sweeps along the gradually increasing length of the electrode gap thus forming a large plasma plume where it breaks down at threshold length. A new arc then appears and develops according to the same procedure. The solid carbon steel target placed in front of the electrodes is therefore exposed to the flux of the impinging activated species generated in the electrical discharge. The GAD device, easy to operate, is a source of chemically reactive species the nature of which depends on the plasma gas used. Compressed air is led through a bubbling water flask to get water-saturated. The plasma treatment was carried out for different exposure times denoted by t and ranging from 0 to 60 min. The working parameters were identified as the electrode gap: $e = 2$ mm, the distance between electrode neck and the carbon steel surface: $d = 3$ cm, the gas flow rate: $Q = 700$ L h^{-1}, and the nozzle diameter $\Phi = 1$ mm which delivers a cylindrical gas flow. The carbon steel samples were cooled by circulating cold water.

2.2 Analytical techniques

Corrosion resistance was always evaluated for an immersion time in the corroding solution at 25 °C during 24 h. The influence of different solutions was studied (electrolyte, pH).
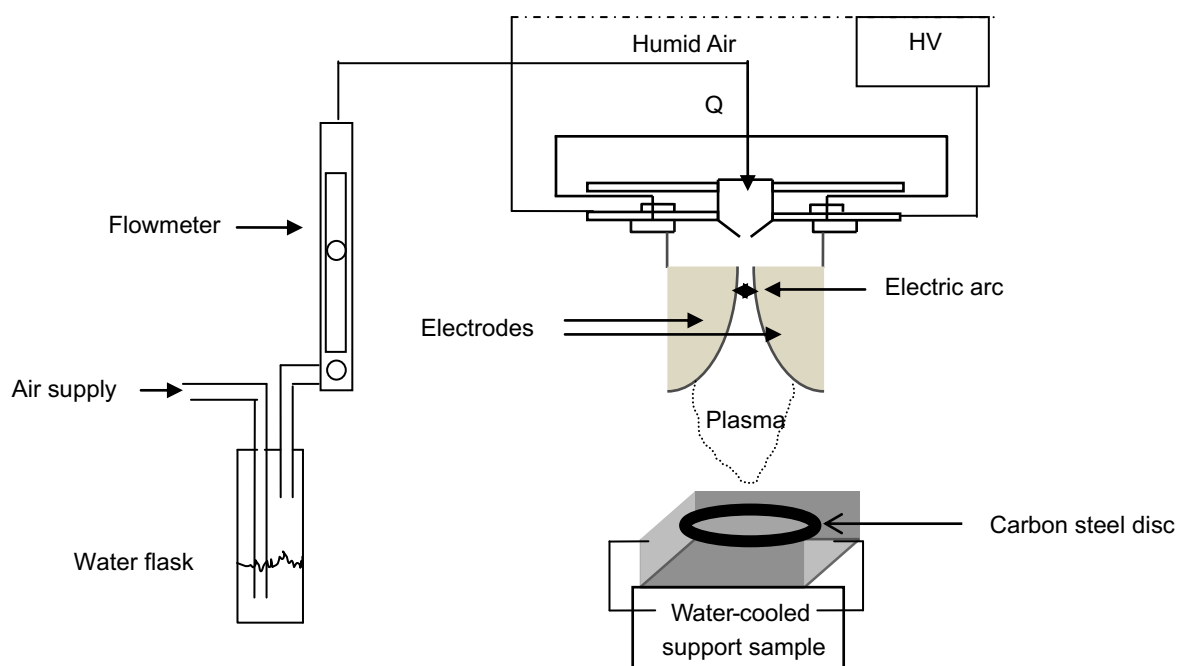

Fig. 1. Gliding arc discharge experimental setup and disposition for treatment of carbon steel.

2.2.1 Gravimetric measurements

Carbon steel samples were 7.55 cm^2 disks. Weight loss tests were carried out in a double-walled glass cell equipped with a thermostat-cooling condenser. The corroding solution (NaCl 0.5 M, pH = 6.4) volume was 100 mL. After the corrosion test (24 h), the specimens of carbon steel were carefully washed in double-distilled water, dried and then weighed. The weight loss was evaluated from the difference between the weight of carbon steel before and after GAD treatment and corrosion test. Weight loss allowed us to calculate the mean corrosion rate denoted by W in mg dm^{-2} day^{-1}.

2.2.2 Polarization curves

Polarization curves were conducted using an electrochemical measurement system potentiostat-galvanostat Voltalab 21 model PGP201 controlled by a PC. The potential of the electrode was swept from its free corrosion potential after 30 min, to more positive values. The test solution was purged with pure nitrogen. Gas bubbling was maintained through the experiments. The working electrode (carbon steel disk 1 ± 0.1 cm^2) was embedded in polytetrafluoroethylene. A conventional three electrode electrochemical cell of volume 100 mL was used. A saturated calomel electrode (SCE) and a platinum disk electrode were used as reference and auxiliary electrodes, respectively. All potentials are reported versus SCE. The linear sweep of potential was set at a speed of 10 mV min^{-1}. The current-potential curves are plotted in the direction of oxidation in the range -1 to 0 V/SCE and displayed directly on the monitor. The corrosion potential E_{corr} and the corrosion current densities i_{corr} are determined on the curve $\log(i) = f(E)$ by Tafel extrapolation method.

2.2.3 Electrochemical impedance spectroscopy (EIS)

EIS tests were performed at room temperature (25 ± 1 °C and pH = 6.4 ± 0.2) in a polymethyl methacrylate cell with a capacity of 1000 mL. A saturated calomel electrode (SCE) was used as the reference; a Pt electrode was used as the counter one. All potentials are reported versus SCE. EIS measurements were performed using a Solartron SI 1287 electrochemical interface and a Solartron 1255B frequency response analyzer in a frequency range of 10^5 Hz to 10^{-1} Hz with 10 points per decade and a sine wave with 10 mV amplitude to perturb the system. Plasma-treated or untreated carbon steel sample (7.5 ± 0.1 cm^2 disks) was used as working electrode. Impedance data were analyzed and fitted with the simulation software ZView 2.80 equivalent circuit. Impedance diagrams are given in the Nyquist and Bode representations. Values of R_{ct} and C_{dl} obtained from Nyquist plots were studied versus GAD treatment time (t).

3 Results and discussion

3.1 Weight loss measurements

Gravimetric measurements of carbon steel samples were performed versus GAD treatment time (t). The corrosion resistance efficiency ($E1\%$) was calculated by the following relation [22]:

$$E1\% = \frac{W_0 - W}{W_0} \times 100, \qquad (1)$$

where W_0 is the corrosion rate of untreated carbon steel and W is the corrosion rate of treated carbon steel. Results are gathered in Table 1.

The corrosion rate decreases as t increases and the inhibition efficiency reaches 75% for $t = 60$ min giving evidence that surface modifications induced on carbon steel surface by the GAD treatment lead to a layer acting as a good corrosion inhibitor.

### 3.2 Potentiodynamic polarization results

The anodic and cathodic corrosion reactions occurring on polarization of untreated or treated carbon steel after immersion in 0.5 M NaCl at pH = 6.4 were studied through the potentiodynamic polarization measurements. The Tafel extrapolation method was applied to the polarization curves and corrosion parameters data including corrosion current density (i_{corr}), corrosion potential (E_{corr}), cathodic Tafel slope (bc), anodic slope (ba)

Table 1. Gravimetric results of carbon steel corrosion in 0.5 M NaCl (pH = 6.4; 24 h; 25 °C) versus GAD treatment time (t).

t (min)	W (mg dm^{-2} day^{-1})	$E1$ (%)
0	43.99	–
10	41.99	04.54
20	33.99	27.73
30	21.99	50.01
45	15.98	63.67
60	10.99	75.01

Table 2. Evolution of polarization parameters and corrosion resistance efficiencies of carbon steel in NaCl (pH = 6.4; 24 h; 25 °C) versus GAD treatment time (t).

t (min)	$-E_{\mathrm{corr}}$ (mV/SCE)	i_{corr} (μA cm^{-2})	ba (mV dec^{-1})	$-bc$ (mV dec^{-1})	$E2$ (%)
0	671.2	33.04	173.12	038.81	–
5	666.8	17.06	180.63	070.54	48.36
10	656.1	12.54	181.01	476.01	62.04
20	645.4	04.00	169.12	406.43	87.89
30	631.6	03.16	090.53	195.12	90.42
45	613.7	02.12	097.44	202.35	93.57
60	594.2	01.60	072.52	310.73	95.15
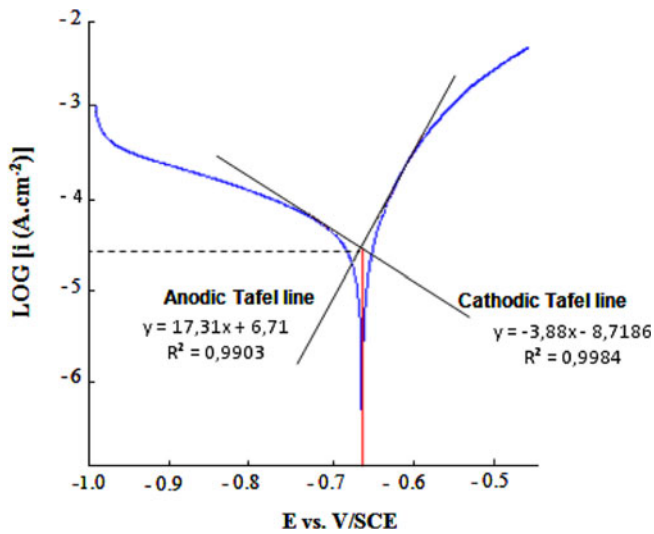
Fig. 2. Tafel curve of non-treated carbon steel in 0.5 M NaCl (pH = 6.4), showing Tafel lines for the determination of corrosion potential and of corrosion current densities (scan rate: 10 mV min^{-1}).

and corrosion resistance efficiency $E2\%$ calculated from equation (2) are listed in Table 2.

$$E2\% = \frac{i_{0corr} - i_{corr}}{i_{0corr}} \times 100, \tag{2}$$

where i_{0corr} and i_{corr} are the corrosion current densities for carbon steel without and with plasma treatment for different exposure times, respectively, determined by extrapolation of cathodic Tafel lines to the corrosion potential. Figure 2 shows the polarization curve obtained for the untreated sample with the Tafel lines.

Electrochemical polarization measurements (Table 2) show that the corrosion current densities decrease as t increases. The potential shift toward the positive direction is due to anodic protection. This effect induces an en-

noblement of corrosion potential of steel. The corrosion potential shift toward the positive direction and the decreasing current density of carbon steel with t indicates the efficiency of the GAD treatment to protect carbon steel against corrosion in 0.5 M NaCl, pH = 6.4 by the formation of a passive film on its surface.

The results of Table 2 show that for $t = 0$ the slope of the Tafel cathodic (bc) polarization curve is -38.8 mV dec^{-1} indicating a strong dissolution of the untreated steel. The increases of bc value versus t imply an increase in the rate of recovery of the formed layer as well as its homogeneity. The active area of the surface of carbon steel is reduced and the formed film may have a resistive behavior. The slope of the Tafel anodic (ba) polarization curve of carbon steel equal to 173.1 mV dec^{-1} for $t = 0$ decreases with t and reaches 72.5 mV dec^{-1} for $t = 60$ min. This decrease is due to the formation of a passivation layer. High efficiency percentages are rapidly reached. It is equal to 87.9% for $t = 20$ min. A decrease in i_{corr} by more than 95.2% is obtained for $t = 60$ min, which proves the efficiency of GAD treatment: the dissolution of GAD treated carbon steel in 0.5 M NaCl, pH = 6.4 is delayed or prevented by the formation of a protective barrier layer. This observation was already made by different authors [9,10] and is consistent with the behavior of an oxide film growing on a metal surface exposed to the corroding plasma gas. The behavior of E_{cor} and i_{corr} as a function of the exposure time to GAD suggests the formation of a protective film, which first causes an increase in the corrosion potential and a decrease in the corrosion current.

3.3 Effect of pH of the solution on the polarization curves of carbon steel treated by plasma

The effect of pH on the electrochemical behavior of carbon steel versus t was evaluated at neutral (pH = 6.4; 0.5 M NaCl) and basic (pH = 11.9; 0.5 M NaCl + 0.006 M NaOH). The pH was adjusted par adding to
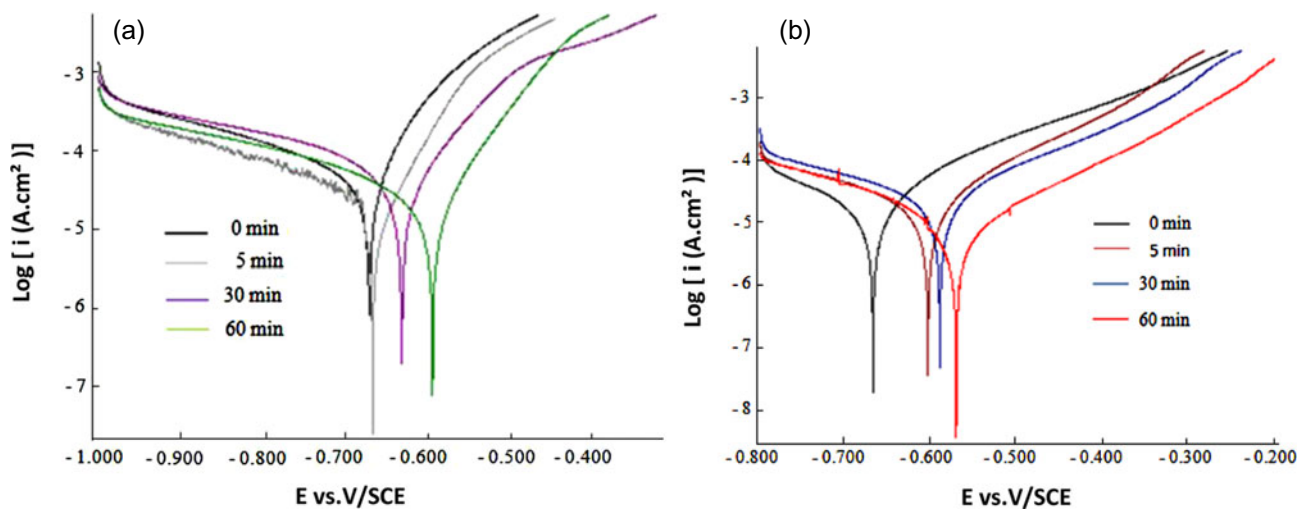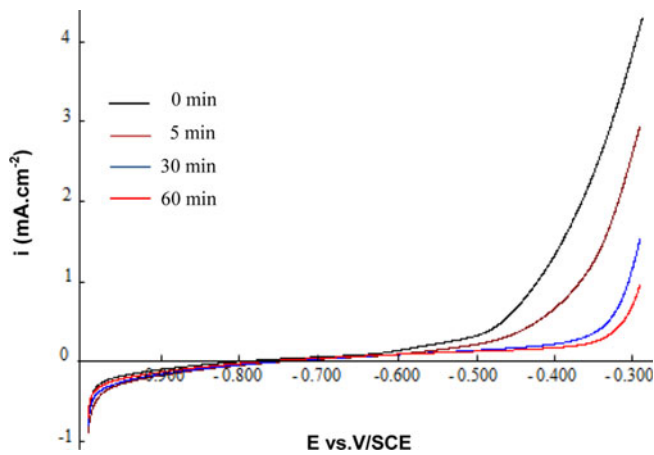

Fig. 3. Polarization curves of carbon steel in 0.5 M NaCl without and with plasma treatment (Fig. 3a: pH = 6.4; Fig. 3b: pH = 1.9; scan rate = 10 mV min^{-1}).
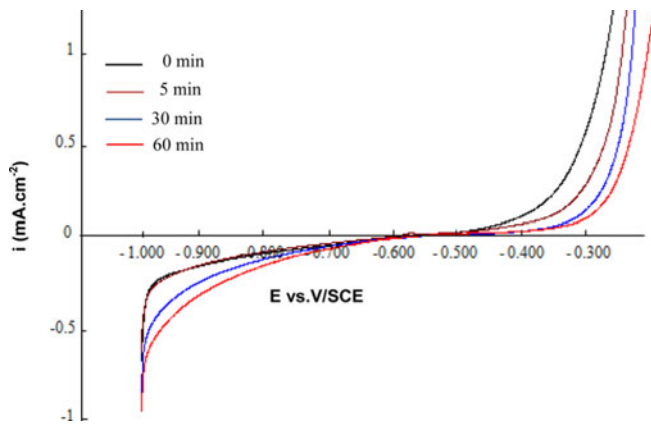
Fig. 4. Voltammograms in (0.5 M NaCl + 0.01 M NaNO₃) of carbon steels exposed to the discharge for 0, 5, 30, 60 min (pH = 6.4).

Fig. 5. Voltammograms in (0.5 M NaCl + 0.01 M NaNO₃ + 0.006 M NaOH) of carbon steels exposed to the discharge for 0, 5, 30, 60 min (pH = 11.9).

NaOH 0.006 M. Results are shown in Figure 3 (pH = 6.4 and 11.9). These results show that the corrosion potential of the steel increases with t and with the pH of the solution. For $t = 60$ min, there is a potential shift to anodic potentials, of 99.5 mV/SCE at pH = 6.4 and of 122 mV/SCE at pH = 11.9 compared to corrosion potential of the untreated carbon steel at pH = 6.4. The corrosion current density decreases with pH of the solution and times duration. This decrease results in the appearance of a larger domain of passivity in alkaline medium, suggesting that the layer formed under plasma is more stable in basic pH.

Similar experiments were performed in another electrolyte and a complexing medium was selected, e.g., (NaCl 0.50 M + NaNO₃ 10^{-2} M) at pH = 6.4 and 11.9 (Figs. 4 and 5). The corrosion potential of steel treated at different exposure times by plasma increases as the pH increases, while corrosion current density decreases. Polarization curves in the complex medium show a larger domain of passivity in the alkaline solution containing nitrate ions. For $t = 60$ min, the voltammogram shows a large passive domain, moving from about 280 mV for at
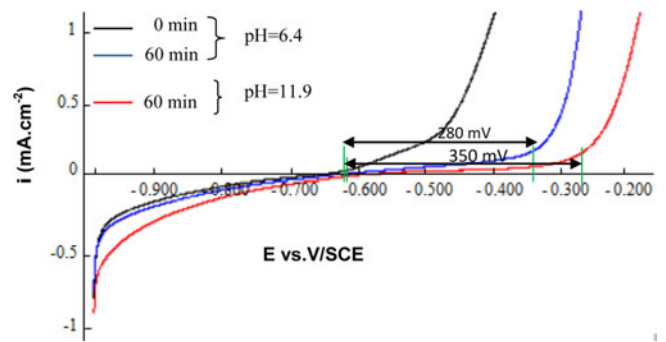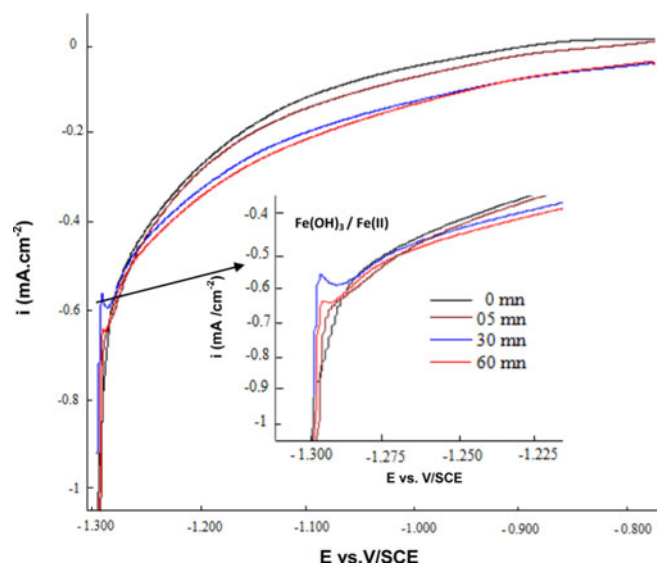

Fig. 6. Voltammograms of carbon steels exposed to the discharge for 60 min. Electrolyze 0.01 M NaNO₃ at different pH (6.5 and 11.9).

pH = 6.4 to about 350 mV for at pH = 11.9 (Fig. 6). This indicates the existence of an oxides/hydroxides layer on carbon steel surface, whose stability is higher at basic pH. In this medium, nitrate ions can be reduced by iron and iron oxide/hydroxide leading to a stable compound layer after a reaction of denitrification already proposed by Hao et al. [23] according to equation (3):

$$8Fe(OH)_2 \downarrow + NO_3^- + 6H_2O \rightarrow NH_3 + 8Fe(OH)_3 \downarrow + OH^- \tag{3}$$
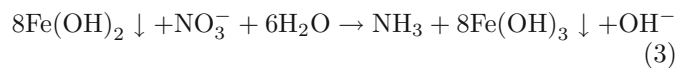
The large passive domain of the treated samples shown by polarization curves in NaCl 0.5 M containing nitrate ions at pH = 11.9 suggests the presence of Fe(II) oxide or hydroxide, as Fe₃O₄ and Fe(OH)₂. The passive layer formed under plasma tends to stabilize in the presence of NO₃⁻ by formation of Fe(OH)₃ on carbon steel surface. This explains larger passive domain observed at pH = 11.9.


Fig. 7. Voltammograms of carbon steel treated at different exposure times to the gliding arc discharge in a NaOH solution of pH = 11.9 (scan rate: 10 mV min⁻¹).

3.4 Reduction of the species formed on the surface of treated carbon steel

The oxides/hydroxides formed on the surface of the carbon steel are reduced in the middle NaOH 0.025 M (pH = 1.7, scan rate 1 V min^{-1}) by linear sweep voltammetry in the potential regime pure diffusion. Cathodic polarization curves of treated carbon steel samples were recorded in 0.025 M NaOH, for various exposure times to the discharges (Fig. 7).

The appearance of a reduction peak to 1.29 V/SCE confirms that the carbon steel surface is oxidized by highly oxidizing species $^\bullet$OH generated by gliding arc discharge. This peak generally corresponds to the reduction of iron hydroxides Fe(OH)$_3$/Fe(II) [10,24]. The reduction poten-

tial of this couple Fe(OH)$_3$/Fe(II) depends on solution pH and potential according to the mechanism [25]:

$$\text{Fe(OH)}_3 + 3\text{e}^- \Leftrightarrow \text{Fe(II)} + 3\text{OH}^- \qquad (4)$$
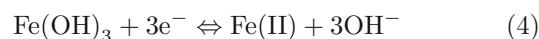
The increase in peak intensity reduction as a function of the exposure time to the discharge reflects an increase in the amount of iron oxides. The peak intensity indicates that the deposited oxide layer is very thin. These results are consistent with the results found by Benstaali et al. [24] for stainless steels (304L and 316L) and Depenyou Jr. et al. [10] for mild steel (AISI 1018).

3.5 Electrochemical impedance spectroscopy (EIS) measurements

The evolution versus t of corrosion behavior of carbon steel was also investigated by EIS for 0.5 M NaCl at room temperature. Nyquist and Bode diagrams were fitted according to the equivalent circuit shown in Figure 8. In this equivalent circuit, R_s, R_{ct} and A represent the solution resistance, the charge transfer resistance and a constant

Fig. 8. Electrochemical equivalent circuit diagram for metal-electrolyte interface.

Table 3. Evolution of EIS characteristic parameters versus treatment time (t) for carbon steel after 24 h immersion in 0.5 M NaCl (pH = 6.4, 24 h, 25 °C).

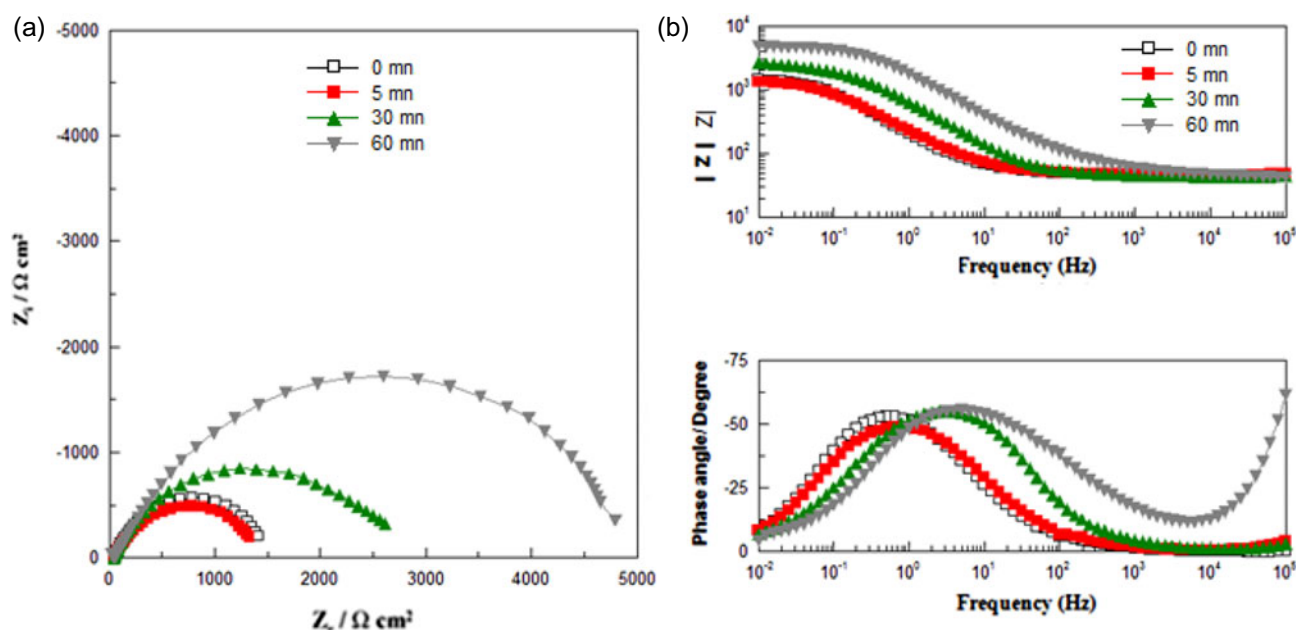| t (min)	R_s (Ω cm^2)	R_{ct} (kΩ cm^2)	n	10^3 A (Ω^{-1} S^n cm^{-2})	C_{dl} (mF cm^{-2})	$E3$ (%)
0	60.17	1.44	0.84	1.19	1.33	–
5	49.36	1.41	0.79	1.67	2.15	–
10	50.23	1.52	0.84	1.09	1.20	4.93
15	46.22	1.68	0.77	0.75	0.80	14.24
30	48.41	2.78	0.79	0.49	0.55	48.11
60	50.02	5.42	0.78	0.63	0.09	73.35

Fig. 9. (a) Nyquist and (b) Bode phase angle diagrams of carbon steel in 0.5 M NaCl without and with plasma treatment.

phase element (CPE) respectively. R_{ct} values were calculated from the difference in impedance at lower and higher frequencies. Corrosion resistance efficiencies ($E3\%$) were calculated using the following formula (5) [26]:

$$E3\% = \left[1 - \frac{R_{\text{ct}}}{R_{\text{ct-treat}}}\right] \times 100, \tag{5}$$

where R_{ct} and $R_{\text{ct-treat}}$ are charge-transfer resistance values for untreated and treated carbon steel respectively. Double layer capacity (C_{dl}) values were calculated in our case by Brug et al. [27], in equation (6).

$$C_{\text{dl}} = \left(A \times R_{\text{ct}}^{1-n}\right)^{1/n}, \tag{6}$$

where A (Ω^{-1} S^n cm^{-2}) is a CPE constant and n is an empirical exponent ($0 \leq n \leq 1$), which measures the deviation from the ideal capacitive behavior. Table 3 shows evolutions of R_{ct}, C_{dl} and $E3\%$ versus t.

Evolutions versus t of Nyquist and Bode diagrams for untreated and treated carbon steel are shown in Figure 9. A decentered capacitive loop from the center of real axis appears. This could be attributed to different physical phenomena such as roughness and heterogeneity of solid surfaces, impurities, grain boundaries and distribution of surface active sites [28,29]. The large peak at 10 Hz frequency and at $50°$ phase angles is associated to the appeared surface layer. The literature [30–33] reports that for porous electrodes, the high frequency response depends on the AC signal penetrability into the pores. When the AC signal does not penetrate as deep as the pores length, it detects only the pores and phase angles between $45°$ and $90°$. The layer obtained gives a great resistance to carbon steel against corrosion. It is clear that the GDA treatment increases the values of R_{ct} and reduces C_{dl}. The decrease in C_{dl} is attributed to an increase of electronic double layer thickness [34]. Increasing R_{ct} value is attributed to the presence of a protective layer on the metal. The data obtained from EIS technique are in good agreement with those obtained from potentiodynamic polarization and mass loss methods.

4 Conclusion

This study gives evidence that highly oxidative property of the $^•$OH radicals modifies the surface sample and forms more resistive barrier layers which improve the corrosion potential and strongly decrease the corrosion current after plasma treatment.

Humid air plasma treatment provokes the corrosion inhibition of carbon steel and gravimetric measurements show that an efficiency equal to 75% is reached for a GAD treatment time equal to 60 min and an immersion in 0.5 NaCl (pH = 6.4) during 24 h. Potentiodynamic polarization measurements indicated that the plasma acts as an anodic inhibitor delaying the corrosion process by forming a protective layer on the surface. The large passive domain of carbon steel treated by plasma shown by polarization curves in NaCl 0.5 M containing nitrate ions at basic pH suggests the presence of Fe(II) oxides/hydroxides,

as Fe_3O_4 and $Fe(OH)_2$. Cathodic polarization curves recorded in 0.025 M NaOH showed the large peak's intensity to 1.29 mV/SCE. This peak generally corresponds to the reduction of iron hydroxides as $Fe(OH)_3$. The increase of the charge transfer resistance of treated carbon steel, reaching 73.3% for $t = 60$ min, confirms the formation and the presence of this layer.

The corrosion inhibition efficiency is really observed on carbon steel surface treated by a GAD plasma. This process which is a clean electric emerging technique could be a good alternative one in order to substitute the toxic chemical inhibitor (benzotriazole) process and consequently in order to preserve and to protect the environment.

References

1. M.M. Mennucci, E.P. Banczek, P.R.P. Rodrigues, I. Costa, Cem. Concr. Compos. **31**, 418 (2009)
2. F. Abdelmalek, M.R. Ghezzar, M. Belhadj, A. Addou, J.L. Brisset, Ind. Eng. Chem. Res. **45**, 23 (2006)
3. F. Abdelmalek, R.A. Torres, E. Combet, C. Petrier, C. Pulgarin, A. Addou, Sep. Purif. Technol. **63**, 30 (2008)
4. E. Njoyim, P. Ghogomu, S. Laminsi, S. Nzali, A. Doubla, J.L. Brisset, Ind. Eng. Chem. Res. **48**, 9773 (2009)
5. M.R. Ghezzar, F. Abdelmalek, M. Belhadj, N. Benderdouche, A. Addou, Appl. Catal. B: Env. **72**, 304 (2007)
6. A. Doubla, L. Bouba Bello, M. Fotso, J.L. Brisset, Dyes Pigm. **77**, 118 (2008)
7. D. Moussa, F. Abdelmalek, B. Benstaali, A. Addou, E. Hnatiuc, J.L. Brisset, Eur. Phys. J. Appl. Phys. **29**, 189 (2005)
8. N. Bellakhal, M. Dachraoui, Mat. Chem. Phys. **85**, 366 (2004)
9. B. Benstaali, A. Addou, J.L. Brisset, Mat. Chem. Phys. **78**, 214 (2002)
10. F. Depenyou Jr., A. Doubla, S. Laminsi, D. Moussa, J.L. Brisset, J.M. Le Breton, Corros. Sci. **50**, 1422 (2008)
11. A. Anders, Surf. Coat. Technol. **200**, 1893 (2005)
12. X. Jiang, X. Xie, X. Zhong, Surf. Coat. Technol. **168**, 156 (2003)
13. J.O. Kamgang, M. Naitali, J.M. Herry, M.N. Bellon-Fontaine, J.L. Brisset, R. Briandet, Plasma. Sci. Tech. **111**, 187 (2009)
14. J. Toshifujia, T. Katsumataa, H. Takikawaa, T. Sakakibaraa, I. Shimizub, Surf. Coat. Technol. **171**, 302 (2003)
15. T. Kosec, D. Kek Merl, I. Milošev, Corros. Sci. **50**, 1987 (2008)
16. K. Draou, N. Bellakhal, B.G. Cheron, J.L. Brisset, Mat. Res. Bull. **33**, 1117 (1998)
17. Z. Ait Chikh, D. Chebabe, A. Dermaj, N. Hajjaji, A. Srhiri, M.F. Montemor, M.G.S. Ferreira, A.C. Bastos, Corros. Sci. **47**, 447 (2005)

18. S. Liu, N. Xu, J. Duan, Z. Zeng, Z. Feng, R. Xiao, Corros. Sci. **51**, 1356 (2009)
19. R. Cabrera-Sierra, E. Sosa, M.T. Oropeza, I. Gonzalez, Electrochim. Acta **47**, 2149 (2002)
20. E.P. Banczek, P.R.P. Rodrigues, I. Costa, Surf. Coat. Technol. **201**, 3700 (2006)
21. H. Lesueur, A. Czernichowski, J. Chapelle, French Patent No. 2 639 172 (1988)
22. H. Amar, A. Tounsi, A. Makayssi, A. Derja, J. Benzakour, A. Outzourhit, Corros. Sci. **49**, 2936 (2007)
23. Z.W. Hao, X.H. Xu, D.H. Wang, J. Zhejiang Univ. Sci. B **3**, 182 (2005)
24. B. Benstaali, J.M. LeBreton, A. Addou, B.G. Cheron, J.L. Brisset, Phys. Chem. News **5**, 87 (2002)
25. J. Sarrazin, M. Verdaguer, *L'oxydoréduction, Concepts et Experiences* (Ellipses, Paris, 1991)
26. M.A. Quraishi, R. Sardar, J. Appl. Electrochem. **33**, 1163 (2003)
27. G.J. Brug, A.L.G. Van den Eeden, M. Sluyters-Rehbach, J.H. Sluyters, J. Electroanal. Chem. **176**, 275 (1984)
28. K. Jüttner, Electrochim. Acta **35**, 1501 (1990)
29. A. Delimi, Y. Coffinier, B. Talhi, R. Boukherroub, S. Szunerits, Electrochim. Acta **55**, 8921 (2010)
30. H.K. Song, Y.H. Jung, K.H. Lee, L.H. Dao, Eletrochim. Acta **44**, 3513 (1999)
31. H.K. Song, H.Y. Hwang, K.H. Lee, L.H. Dao, Eletrochim. Acta **45**, 2241 (2000)
32. I.V. Aoki, M.C. Benard, S.I. Cordoba de Torresi, C. Deslouis, H.G. De Melo, S. Joiret, B. Tribollet, Eletrochim. Acta **46**, 1871 (2001)
33. I. Costa, M.C.L. Oliveira, H.G. Melo, R.N. Faria, J. Magn. Mater. **278**, 348 (2004)
34. M.G. Hosseini, M. Ehteshamzadeh, T. Shahrabi, Electrochim. Acta **52**, 3680 (2007)